

# Investigation of the interaction of some astrobiological molecules with the surface of a graphite (0001) substrate. Application to the CO, HCN, H<sub>2</sub>O and H<sub>2</sub>CO molecules.

Azzedine Lakhelif\*

John P. Killingbeck†

November 19, 2018

## Abstract

Detailed semi-empirical interaction potential calculations are performed to determine the potential energy surface experienced by the molecules CO, HCN, H<sub>2</sub>O and H<sub>2</sub>CO, when adsorbed on the basal plane (0001) of graphite at low temperature. The potential energy surface is used to find the equilibrium site and configuration of a molecule on the surface and its corresponding adsorption energy. The diffusion constant associated with molecular surface diffusion is calculated for each molecule.

## 1 Introduction

Observations in the cold regions of the interstellar medium (ISM) with typical temperatures of about 10 - 20 K have revealed the presence of clouds which contain high densities (more than  $10^3$  particle per  $\text{cm}^3$ ) of atoms, radicals and simple molecules such as H<sub>2</sub>, CO, CO<sub>2</sub>, HCN, H<sub>2</sub>O (the most abundant molecule), NH<sub>3</sub>, H<sub>2</sub>CO, CH<sub>4</sub>, CH<sub>3</sub>OH, as well as small solids typically composed of amorphous H<sub>2</sub>O, silicates and carbon grains in the form of graphite, amorphous structures and polycyclic aromatic hydrocarbon (PAH) molecules [1, 2].

It is nowadays thought that the dominant mechanism for the formation of molecules is provided by surface-catalysed chemical reactions on low temperatures interstellar dust grains. For instance, Watanabe and Kouchi [3] have experimentally produced the formaldehyde H<sub>2</sub>CO and methanol CH<sub>3</sub>OH molecules by successive hydrogenation of CO on the surface of icy grains at 10 K, as was theoretically proposed by Tielens et al. [4]. Recent laboratory experiments reported that more complex molecules such as glycine and other amino acids (which play an important role in the origin and evolution of life) as well as other organic species were formed from ultraviolet (UV) irradiation of the analogues of icy interstellar grains at low temperatures ( $T \sim 15$  K) and containing small amounts of HCN, NH<sub>3</sub>, H<sub>2</sub>CO, and CH<sub>3</sub>OH species [5, 6].

Theoretical quantum-chemical calculations on the synthesis of amino acids were reported by Woon [7] for UV-irradiated astrophysical ices and by Mendoza et al. [8] for ice analogues on the surface of a coronene (PAH) molecule.

Investigations of the chemical processes leading to the production of amino acids on the surface of grains require a knowledge of the interactions between the molecules participating in these processes

---

\*Institut Universitaire de Technologie, Belfort-Montbéliard.

E-mail : azzedine.lakhelif@obs-besancon.fr

Institut Utinam - UMR CNRS 6213 Université de Franche-Comté Observatoire de Besançon

41 bis avenue de l'Observatoire - BP 1615 - 25010 Besançon Cedex, France

†Mathematics Department, University of Hull, Hull HU6 7RX, UK

on the surface, and also of their adsorption characteristics (such as the equilibrium configurations and diffusion constants) when they are isolated on the grain surface.

The interaction of a single water molecule with a graphite sheet and with PAH molecules like the fused-benzene molecules (fbz)<sub>n</sub> (C<sub>6</sub>H<sub>6</sub>, C<sub>24</sub>H<sub>12</sub>, C<sub>54</sub>H<sub>18</sub>, C<sub>96</sub>H<sub>24</sub>,... for  $n = 1, 7, 19, 37, \dots$ , respectively) has been theoretically studied using *ab-initio* methods to determine the binding energies and equilibrium configurations [9, 10, 11, 12, 13, 14, 15, 16]. For H<sub>2</sub>O adsorbed on a graphite sheet, the calculated binding energies by various authors are -187 [10], -72 [9], and -109 meV [17]. The available experimental value is -156 meV [18].

For the water-benzene complex, many theoretical *ab-initio* calculations were reported. The calculated binding energies are around -120 [15, 16, 14], -169 meV [11], and -99 meV [13]. The available experimental values are -98 [19], and -106 meV [20].

Feller and Jordan [12] have reported for water-(fbz)<sub>n</sub> complex up to  $n = 37$  an energy binding -251 meV which is twice as large as the recently reported value -126 meV by Lin et al. [13].

In the present work we study the adsorption properties of several of the molecules which are associated with the synthesis of amino acids. We use the graphite (0001) surface as a model substrate to represent the surface of an interstellar dust grain and we consider the surface adsorption of the various molecules on the model surface. We use an approach which has already been developed to calculate the infrared spectra of the NH<sub>3</sub> ammonia molecule adsorbed on a variety of surfaces [21, 22, 23, 24]. The basic procedure involves the calculation of the potential energy surface for the adsorbed molecule as it moves on the adsorbing surface. The environmental effect on the inversion spectrum of NH<sub>3</sub>, for example, can be simulated by changes in the depth or curvature of an effective double well potential. Depending on the substrate surface it may happen that, for the NH<sub>3</sub> molecule, the central barrier height increases (giving reduced splittings within each of the lowest two vibrational levels) or an asymmetry appears between the two potential wells. Even a slight asymmetry can inhibit the inversion motion in NH<sub>3</sub>, so that the eigenstates are effectively localized on one side or the other of the central potential barrier. These earlier calculations with NH<sub>3</sub> have given us experience of the calculational techniques involved and they led to calculated spectra which were in agreement with the experimental ones.

The isosteric heat of adsorption for NH<sub>3</sub> adsorbed on the graphite substrate calculated in our model was 178 meV [24], in agreement with the experimental value of 172 meV given by Avgul and Kiselev [18] at a temperature  $T = 195$  K.

The various parts of section 2 of this work describe the important contributions to the potential energy of the adsorbed molecule on the adsorbing surface. Section 3 describes the minimization process needed to find the possible equilibrium positions of the adsorbed molecule on the surface and gives details of the observables which are to be calculated. Section 4 gives the results obtained for the several molecules studied; typical potential surfaces are shown in the figures, to augment the sometimes complicated verbal description of the equilibrium positions of the molecule.

Two tables set out some important calculated numerical parameters for the various adsorbed molecules. An appendix sets out some of the mathematical transformations needed to transform various quantities between the internal molecular axes and the chosen reference set of axes needed to give a unified description of the various quantities.

## 2 Theoretical background

An adsorbed species can be either physically or chemically bonded to the surface of the substrate crystal. In physisorption the interaction is due to the comparatively weak van der Waals-London and electric field-multipole forces, and the interaction potential energy is fairly low ( $\leq 0.5$  eV), with no charge exchange between the adsorbed species and the substrate.

### 2.1 The physisorbed molecule on a graphite substrate

In this work we consider a single molecule such as CO, HCN, H<sub>2</sub>O or H<sub>2</sub>CO physisorbed on a graphite basal plane (0001) at low temperatures.

The graphite crystal is extensively used as a model to simulate the behaviour of interstellar grains in studies of the physical and chemical behaviour of adsorbed molecular species. Experimentally detected

absorption features due to carbon grains have been attributed to the presence of small spherical graphite crystals of size  $\sim 200 \text{ \AA}$  in interstellar dust clouds [1, 2].

In order to reduce the required numerical calculation times, the graphite crystal is modelled by using ten planes with radii  $\sim 35 \text{ \AA}$  ( $\sim 1500$  carbon atom per plane). This does not significantly influence the interaction potential energy between the molecule and the substrate (giving an error of less than 2 percent).

Figure 1 shows the geometrical characteristics of a molecule ( $\text{H}_2\text{CO}$  for instance) adsorbed on the graphite surface.

To perform the calculations, we need to define:

*i*) an absolute frame ( $\mathbf{O}, \mathbf{X}, \mathbf{Y}, \mathbf{Z}$ ) connected to the surface of the substrate, with respect to which all of the vectors and the tensors associated with the molecule and the graphite carbon atoms must be described;

*ii*) a frame ( $\mathbf{G}, \mathbf{x}, \mathbf{y}, \mathbf{z}$ ) tied to the molecule with centre of mass  $\mathbf{G}$ , and with respect to which the molecular vibrational motions are still described. The rotational matrix transformation from the absolute frame to the molecular frame is given in Appendix A, in terms of the molecular orientational degrees of freedom  $\Omega = (\varphi, \theta, \chi)$  (precession, nutation, and proper rotation Euler angles).

## 2.2 Interaction potential energy

The interaction potential energy  $V_{\text{MG}}$  between an adsorbed molecule and the graphite substrate can be written as the sum of three parts

$$V_{\text{MG}} = V_{\text{LJ}} + V_{\text{E}} + V_{\text{I}}, \quad (1)$$

which are detailed below.

### 2.2.1 Quantum contributions

The first term  $V_{\text{LJ}}$  in Eq. (1) is generally treated by using semi-empirical 12-6 Lennard-Jones (LJ) pairwise atom-atom potentials to describe the short-range atomic repulsion energy arising from the overlap of the electronic clouds of the adsorbate and the substrate at very short distances and also the long-range many-body dispersion energy arising from the lowering of the quantum zero-point energy of the system by the correlated fluctuations of the adsorbate and substrate atomic dipoles.

However, it is widely known that carbon atoms in the graphite basal plane (0001) exhibit anisotropic polarizability effects which modify the spherical shape of these atoms. To account for these anisotropies, Carlos and Cole [25] proposed a modified expression for  $V_{\text{LJ}}$ , of the form

$$V_{\text{LJ}} = \sum_j \sum_i 4\epsilon_{ij} \left\{ \left( \frac{\sigma_{ij}}{|\mathbf{r}_{ij}|} \right)^{12} \left[ 1 + \gamma_R \left( 1 - \frac{6}{5} \cos^2 \theta_{ij} \right) \right] - \left( \frac{\sigma_{ij}}{|\mathbf{r}_{ij}|} \right)^6 \left[ 1 + \gamma_A \left( 1 - \frac{3}{2} \cos^2 \theta_{ij} \right) \right] \right\}. \quad (2)$$

In this equation,  $\mathbf{r}_{ij}$  is the distance vector between the  $i$ th atom of the molecule and the  $j$ th carbon atom of the graphite substrate (Figure 1), while  $\epsilon_{ij}$  and  $\sigma_{ij}$  are the mixed LJ potential parameters, obtained from the usual Lorentz-Berthelot combination rules  $\epsilon_{ij} = \sqrt{\epsilon_{ii}\epsilon_{jj}}$  and  $2\sigma_{ij} = \sigma_{ii} + \sigma_{jj}$ . The two coefficients  $\gamma_R$  and  $\gamma_A$  specify the modifications to the repulsion and dispersion parts of the energy, respectively, and  $\theta_{ij}$  is the angle between the surface normal axis and the  $\mathbf{r}_{ij}$  vector. The various molecule-graphite mixed parameters are given in Table 1. Note that the LJ parameters used in this work have been improved several times in our other works.

### 2.2.2 Electrostatic and induction contributions

It is well known that the bonds in the graphite crystal give rise to aspherical atomic charge distributions which produce multipole electrostatic fields with rapid spatial variations external to the graphite [9]. This phenomenon is modelled by introducing axially symmetric quadrupole moment tensors  $\Theta^c$  at each carbon atom site.

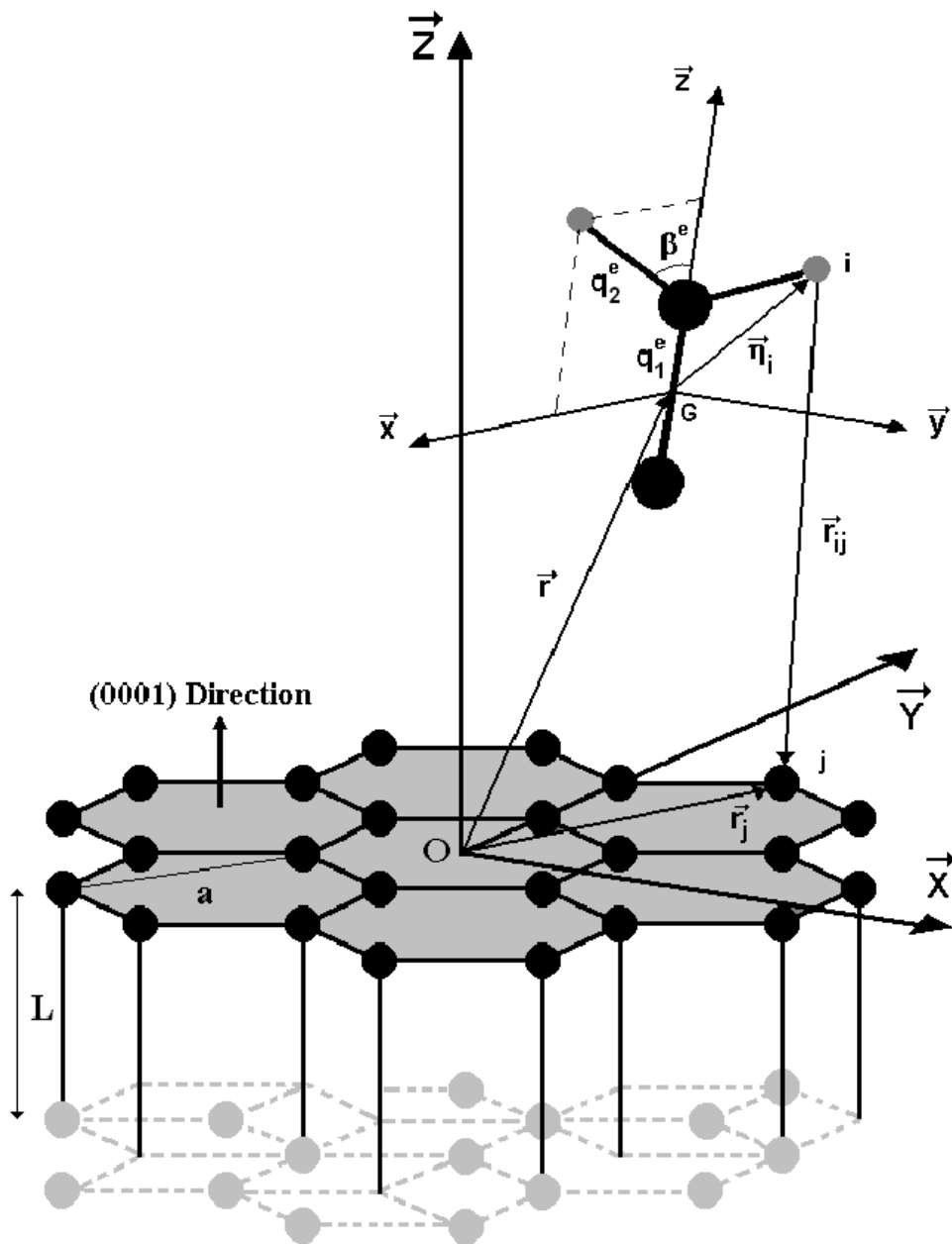


Figure 1: Geometrical characteristics of an  $\text{H}_2\text{CO}$  molecule adsorbed on the graphite (0001) substrate.  $(\mathbf{O}, \mathbf{X}, \mathbf{Y}, \mathbf{Z})$  and  $(\mathbf{G}, \mathbf{x}, \mathbf{y}, \mathbf{z})$  represent the surface absolute frame and the molecular frame, respectively.  $L$  and  $a$  are the interlayer spacing and the distance between two next-nearest neighbour carbon atoms of the graphite and  $q_1^e$ ,  $q_2^e$  and  $\beta^e$  define the equilibrium internal coordinates of the adsorbed molecule.

Table 1: Lennard-Jones parameters for atom-graphite combinations.

Gr - Atom	$\epsilon$ (meV)	$\sigma$ (Å)	$\gamma_A^{(a)}$	$\gamma_R^{(a)}$
Gr - H	2.265	2.965	0.4	-0.54
Gr - O	3.450	3.141	0.4	-1.05
Gr - C	2.981	3.305	0.4	-1.05
Gr - N	2.811	3.390	0.4	-1.05

(a) From Refs. [25, 26, 27, 28, 29].

The quadrupole moment tensor  $\Theta^c$  of the  $j$ th carbon atom produces the electrical potential

$$\Phi^j(\mathbf{r}) = \frac{1}{3}L_p \times \nabla \nabla \left( \frac{1}{|\mathbf{r}_j - \mathbf{r}|} \right) : \Theta^c, \quad (3)$$

on the molecule at its centre of mass position  $\mathbf{r}$ . In turn, the multipole moments  $(\mu, \Theta, \dots)$  of the molecule produce the electrical potential

$$\Phi^M(\mathbf{r}_j) = L_p \times \nabla \left( \frac{1}{|\mathbf{r}_j - \mathbf{r}|} \right) \cdot \mu + \frac{1}{3}L_p \times \nabla \nabla \left( \frac{1}{|\mathbf{r}_j - \mathbf{r}|} \right) : \Theta + \dots, \quad (4)$$

on the  $j$ th carbon atom at position  $\mathbf{r}_j$ .

In Eqs. (3) and (4),  $L_p$  is a screening factor, equal to 1 for the surface plane and to  $2/(\epsilon + 1)$  for the internal planes ( $p \geq 2$ ), where  $\epsilon$  is the static dielectric constant of the graphite crystal, which we take to be 2.8.

The electrostatic and induction contributions to the interaction potential energy  $V_{MG}$  are

$$V_E = \sum_j \mu \cdot \nabla \Phi^j(\mathbf{r}) + \frac{1}{3} \sum_j \Theta : \nabla \nabla \Phi^j(\mathbf{r}) + \dots \quad (5)$$

$$V_I = -\frac{1}{2} \sum_j [\nabla \Phi^M(\mathbf{r}_j) : \alpha^c : \nabla \Phi^M(\mathbf{r}_j)] - \frac{1}{2} \sum_{j,j'} [\nabla \Phi^j(\mathbf{r}) : \alpha : \nabla \Phi^{j'}(\mathbf{r})], \quad (6)$$

where  $\alpha$  and  $\alpha^c$  are the polarizability tensors of the molecule and of the graphite carbon atoms, respectively.

The elements of the polarizability  $\alpha^c$  and quadrupole moment  $\Theta^c$  tensors (Eqs. (3-6)) of the carbon atoms are given in the absolute frame  $(\mathbf{O}, \mathbf{X}, \mathbf{Y}, \mathbf{Z})$  by

$$\alpha_{XX}^c = \alpha_{YY}^c = \alpha_{\perp}^c \quad \text{and} \quad \alpha_{ZZ}^c = \alpha_{\parallel}^c, \quad (7)$$

$$\Theta_{XX}^c = \Theta_{YY}^c = -\frac{1}{2}\Theta_{ZZ}^c = -\frac{1}{2}\Theta^c, \quad (8)$$

with all other elements being zero.

Moreover, it must be noticed that the molecular frame corresponds, for each of the studied molecules, to its principal frame of inertia, in which only the  $z$ -component of the dipole moment  $\mu$  vector and the three diagonal elements of the polarizability  $\alpha$  and quadrupole moment  $\Theta$  tensors are non-vanishing elements. In the potential energy calculations these quantities must be expressed in the absolute frame by using a rotational matrix transformation (Appendix A).

The various geometrical and electrical parameters of the graphite substrate and of the studied molecules are given in Table 2.

### 2.2.3 Separation of $V_{MG}$

The distance vector  $\mathbf{r}_{ij}$  in Eq. (2) can be expressed as

$$\mathbf{r}_{ij} = \mathbf{r}_j - \mathbf{r} - \eta_i, \quad (9)$$

Table 2: Molecular and graphite parameters: internal bonds and angles, dipole moments, polarizabilities, quadrupole moments, and rotational constants for the molecules studied.

Molecule	CO	HCN	H <sub>2</sub> O	H <sub>2</sub> CO	Graphite <sup>(a)</sup>	
{q <sup>e</sup> } (Å)	1.144	1.150	0.958	1.198	$L$ (Å)	3.36
	-	1.079	-	1.121	$a$ (Å)	2.46
$\beta^e$ (deg)	-	-	54.7	58.1		
$\mu$ (D)	0.112	2.986	1.855	2.330		
$\alpha_{xx}$ (Å <sup>3</sup> )	1.63	2.05	1.53	2.51	$\alpha_{\perp}^c$ (Å <sup>3</sup> )	1.44
$\alpha_{yy}$ (Å <sup>3</sup> )	1.63	2.05	1.42	1.94	$\alpha_{\parallel}^c$ (Å <sup>3</sup> )	0.41
$\alpha_{zz}$ (Å <sup>3</sup> )	2.60	3.66	1.47	2.90		
$\Theta_{xx}$ (DÅ)	1.02	-2.20	2.63	1.91	$\Theta^c$ (DÅ)	1.0
$\Theta_{yy}$ (DÅ)	1.02	-2.20	-2.50	-5.01		
$\Theta_{zz}$ (DÅ)	-2.05	4.40	-0.13	3.09		
A (cm <sup>-1</sup> )	1.93	1.48	27.33	1.22		
B (cm <sup>-1</sup> )	1.93	1.48	14.57	1.13		
C (cm <sup>-1</sup> )	-	-	9.49	9.40		

(a) From Refs. [25, 26, 27, 28, 29].

where  $\mathbf{r}$  and  $\mathbf{r}_j$  are the position vectors of the molecular centre of mass and the  $j$ th graphite carbon atom, respectively.

The vectors  $\eta_i$  characterize the positions of the atoms in the molecule. They, as well as the molecular electrical parameters  $\mu$ ,  $\Theta$ ,  $\alpha$ , depend on the molecular internal vibrational motions. They could be written, with respect to the (G,x,y,z) frame, as

$$\begin{aligned}
 \eta_i &= \eta_i^e + \sum_{\nu} \mathbf{a}_i^{\nu} Q_{\nu} + \dots, \\
 \mu &= \mu^e + \sum_{\nu} \mathbf{b}^{\nu} Q_{\nu} + \dots, \\
 \Theta &= \Theta^e + \sum_{\nu} \mathbf{c}^{\nu} Q_{\nu} + \dots, \\
 \alpha &= \alpha^e + \sum_{\nu} \mathbf{d}^{\nu} Q_{\nu} + \dots
 \end{aligned} \tag{10}$$

In these expressions the superscript e refers to the equilibrium internal configuration of the molecule (rigid molecule) and  $\mathbf{a}_i^{\nu}$ ,  $\mathbf{b}^{\nu}$ ,  $\mathbf{c}^{\nu}$ , and  $\mathbf{d}^{\nu}$  are the first derivatives of  $\eta_i$ ,  $\mu$ ,  $\Theta$ , and  $\alpha$  with respect to the normal coordinate  $Q_{\nu}$  associated with the  $\nu$ th molecular vibrational mode with frequency  $\omega_{\nu}$ .

However, the present work is devoted to finding the adsorption energies and diffusion constants of single molecules adsorbed on the graphite substrate. Therefore, we can assume: *i*) the substrate to be rigid ( $\{\mathbf{r}_j\} = \{\mathbf{r}_j^e\}$ ), *ii*) the adiabatic approximation to be valid, permitting us to separate the high frequency vibrational modes of the molecule from its low frequency external translational and orientational modes, and *iii*) the dynamical coupling between all of the molecular and the graphite degrees of freedom to be negligible.

The interaction potential energy  $V_{\text{MG}}$  can then be written as

$$V_{\text{MG}} = V_{\text{MG}}(\mathbf{r}, \Omega, \{Q_{\nu}^e\}) + V_{\text{MG}}(\{Q_{\nu}\}, \mathbf{r}^e, \Omega^e), \tag{11}$$

where  $V_{\text{MG}}(\mathbf{r}, \Omega, \{Q_{\nu}^e\})$  represents the external motion-dependent part of the potential energy experienced by the non-vibrating molecule.  $V_{\text{MG}}(\{Q_{\nu}\}, \mathbf{r}^e, \Omega^e)$  characterizes the vibrational dependent part, for the molecule at its equilibrium position and orientation; in a perturbative approach it contributes to the molecular gas phase vibrational Hamiltonian and leads to small vibrational frequency shifts.

### 3 Adsorption observables

At sufficiently low temperatures and within the rigid molecule and substrate approximation, the potential energy surface  $V_{\text{MG}}(X, Y)$ , which is experienced by the adsorbed molecule as it moves laterally above the surface can be calculated by minimizing  $V_{\text{MG}}$  with respect to both the perpendicular distance  $Z$  between the molecular centre of mass and the surface and the molecular angular coordinates  $(\varphi, \theta, \chi)$ .

The resulting energy map gives information about the equilibrium site  $(r^e, \Omega^e)$ , and the lateral diffusion valley leading from one equilibrium site to an adjacent one. This makes it possible to determine the isosteric heat of adsorption or adsorption energy and also the surface diffusion constant.

#### 3.1 Adsorption energy

The isosteric heat of adsorption  $E_a$  of a single adsorbed molecule on the graphite substrate can be defined as the energy required to keep the molecule with thermal energy  $(\frac{n}{2} + 1)kT$  at its equilibrium configuration on the surface of the substrate. It is approximately expressed as

$$E_a \simeq \left(\frac{n}{2} + 1\right) kT - V_{\text{MG}}^m(r^e, \Omega^e) - \sum_{s=1}^n \frac{\hbar\omega_s}{2} \coth\left(\frac{\hbar\omega_s}{2kT}\right), \quad (12)$$

where  $n$  is the number of external degrees of freedom for the molecule (5 for linear molecules and 6 for non linear molecules) and  $k$  is the Boltzmann constant. The  $\omega_s$  ( $s=1$  to  $n$ ) are the frequencies associated with the translational and orientational motions of the molecule around their equilibrium positions.

#### 3.2 Surface diffusion constant

Let  $V_{\text{MG}}(\tau, \xi_\gamma(\tau))$  be the instantaneous potential energy surface experienced by the adsorbed molecule with mass  $m$  as it moves along the diffusion valley described by the coordinate path  $\tau$ .  $\xi_\gamma(\tau)$  describe the instantaneous distance from the surface ( $\gamma = Z$ ) and the instantaneous orientation ( $\gamma = \varphi, \theta, \chi$ ) of the molecule for the given  $\tau$  value.

If we disregard the dynamics of the  $\xi$  degrees of freedom around their  $\tau$ -dependent equilibrium values  $\hat{\xi}$  along the diffusion motion of the molecule and use the classical transition state theory [30], then the jumping rate for the diffusion from one equilibrium site  $S_1$  to an equivalent adjacent one  $S_2$  can be written as [31]

$$K(T) \simeq \left(\frac{kT}{2\pi m^*}\right)^{\frac{1}{2}} \frac{\exp[-\Delta V_{\text{MG}}(\tau_0)/kT]}{\int_{\tau_1}^{\tau_2} d\tau \exp[-\Delta V_{\text{MG}}(\tau)/kT]}, \quad (13)$$

where  $\Delta V_{\text{MG}}(\tau) = V_{\text{MG}}(\tau) - V_{\text{MG}}(\tau_1)$ , and  $\tau_0$  corresponds to the saddle point position along the diffusion valley. The diffusion constant is then

$$D(T) = \lambda^2 K(T), \quad (14)$$

where  $\lambda = \tau_2 - \tau_1$  is the jump length, i.e., the distance (in the diffusion direction) between the two adjacent equilibrium sites.

In Eq. (13)  $m^*$  is an effective molecular mass which is due to an inertial effect resulting from the changes in the distance of the molecule from the surface and in the molecules orientation as the diffusion process proceeds. It is expressed as

$$m^* = m \left(1 + \sum_{\gamma} \frac{A_{\gamma}}{m} \hat{a}_{\gamma}^2\right), \quad (15)$$

where  $A_\gamma$  represents the molecular mass  $m$  for  $\gamma = Z$  and the molecular moments of inertia  $I_a$ ,  $I_b$ , and  $I_c$  for  $\gamma = \varphi$ ,  $\theta$ , and  $\chi$ , respectively. The  $\hat{a}_\gamma = \frac{\partial \hat{\xi}_\gamma}{\partial \tau}$  represent deformation parameters as the molecule migrates from an equilibrium site to the saddle point position along the diffusion valley.

## 4 Numerical results

### 4.1 Potential energy surfaces and equilibrium configurations

The potential energy surfaces  $V_{\text{MG}}(X, Y)$  for the CO, HCN, H<sub>2</sub>O, H<sub>2</sub>CO single molecules adsorbed on the graphite substrate are presented in Figures 2 using a square surface area of  $(a \times \frac{2a}{\sqrt{3}})$ , where the lattice parameter  $a$  is shown in Figure 1.

In Table 3 we give, for each adsorbed species, some characteristics of the adsorption, such as the most favourable positions and orientations and their associated energy minima  $V_{\text{MG}}^{\text{m}}$ , as well as the energy maxima  $V_{\text{MG}}^{\text{M}}$ .

#### 4.1.1 CO admolecule

The potential energy surface experienced by the CO adsorbed molecule is presented in Figure 2a. The molecule exhibits an equilibrium configuration with an associated energy minimum  $V_{\text{MG}}^{\text{m}} = -120.2$  meV located above the hexagon site centre at a distance  $Z = 3.08$  Å from the surface and for a nearly flat orientation ( $\theta^e \simeq 95$  deg) position.

The perpendicular orientational motion around this equilibrium configuration is a librational motion with an energy barrier height of about 40 meV, while that in the plane parallel to the surface ( $\varphi$ ) is a free rotational motion.

The energy maximum  $V_{\text{MG}}^{\text{M}} = -106.5$  meV is obtained with the molecule in a nearly flat configuration at a distance  $Z = 3.24$  Å above the graphite carbon sites. There is a surface corrugation energy  $V_{\text{MG}}^{\text{M}} - V_{\text{MG}}^{\text{m}} = 13.7$  meV.

The saddle point of the diffusion path is reached when the molecular centre of mass is above the middle of the carbon-carbon bonds at  $Z = 3.20$  Å from the surface, with the molecule perpendicular to the C-C bonds and being always in the nearly flat configuration (Figure 3a). The associated energy barrier height is  $\Delta V_{\text{MG}}(\tau_0) = 12$  meV (Table 6).

#### 4.1.2 HCN admolecule

The linear HCN adsorbed molecule presents a potential energy surface with six most favourable sites per graphite hexagon (Figure 2b). The energy minimum  $V_{\text{MG}}^{\text{m}} = -175.5$  meV is reached with the molecule in a nearly flat configuration ( $\theta^e \simeq 100$  deg) with its centre of mass at  $Z = 3.20$  Å on the half of the C-C bonds, with a displacement of 0.28 Å inside the hexagon surface and with the hydrogen atom of the molecule pointing in the hexagon site centre direction.

In these equilibrium sites there is a strongly hindered orientational motion perpendicular to the surface ( $\theta$  motion) with an energy barrier height of about 75 meV and a moderately hindered parallel one ( $\varphi$  motion) with an energy barrier height of about 16 meV.

However, it is interesting to note that this latter orientational motion, combined with the translation motion of the molecule between the six equilibrium sites along a quasi-circular trajectory of radius  $\simeq 0.95$  Å around the hexagon site centre, could be regarded as a quasi-free motion (Figure 3b) with an energy barrier height  $\leq 1.5$  meV. Thus, an associated effective moment of inertia must be defined with respect to a new HCN y-axis lying at 0.95 Å from its centre of mass (between the C and H atoms).

The energy maximum of  $V_{\text{MG}}^{\text{M}} = -162.5$  meV is obtained with the molecular centre of mass at  $Z = 3.24$  Å, nearly above the hexagon site centre and also with the nearly flat configuration. This induces a surface corrugation energy of 13 meV.

Table 3: Adsorption characteristics for CO, HCN, H<sub>2</sub>O and H<sub>2</sub>CO molecules.

Molecule	$X^e$ (Å)	$Y^e$ (Å)	$Z^e$ (Å)	$\varphi^e$ (deg)	$\theta^e$ (deg)	$\chi^e$ (deg)	$V_{MG}^m$ (meV)	$V_{MG}^M$ (meV)
CO	0.	0.	3.08	free	95	-	- 120.0	- 106.5
HCN	- 0.95	0.	3.20	0	103	-	- 175.5	- 162.5
H <sub>2</sub> O	- 1.23	- 0.36	3.00	90	100	90	- 138.0	- 129.5
H <sub>2</sub> CO	- 1.11	0.	3.04	0	90	90	- 208.5	- 186.5

Moreover, this position also corresponds to the saddle point of the diffusion motion from one equilibrium site of a hexagon to one equivalent equilibrium site of an adjacent hexagon (Figure 3b).

#### 4.1.3 H<sub>2</sub>O admolecule

The potential energy surface of the non-linear H<sub>2</sub>O molecule adsorbed on the graphite substrate is presented in figure 2c. The most favourable sites are obtained for the molecular centre of mass at  $Z = 3.00$  Å above the C-C bonds, with a displacement of 0.36 Å from the C graphite carbon atom, the oxygen atom of the molecule being always close to this C graphite carbon atom (Figure 3c).

The energy minimum  $V_{MG}^m = -138.0$  meV is obtained with the molecule in a nearly flat configuration ( $\theta^e \simeq 100$  deg and  $\chi = \frac{\pi}{2}$ ) and sitting astride the C-C bonds (Table 3), and is in agreement with the available experimental value -156 meV obtained by Avgul and Kiselev [18].

It should be noted that in the equilibrium sites the angular motions of the C<sub>2</sub> molecular symmetry axis (z-axis) parallel ( $\varphi$  motion) and perpendicular ( $\theta$  motion) to the surface around their equilibrium values are moderately hindered motions with energy barrier heights of about 8 and 15 meV, respectively. The angular (spinning) motion about this axis ( $\chi$  motion) is a completely hindered motion, the energy barrier height being about 400 meV.

The energy maximum  $V_{MG}^M = -129.5$  meV is reached for  $Z = 2.92$  Å above the hexagon site centre with the C<sub>2</sub> molecular symmetry axis perpendicular to the surface of the graphite substrate. The surface corrugation energy is then 8.5 meV.

In Figure 3c we sketch the valley of diffusion of the water molecule on the surface. The barrier height at the saddle point is  $\Delta V_{MG}(\tau_0) = 1$  meV (Table 6). Note however, that to obtain such a motion it is necessary to combine the translational motion and a reorientational motion parallel to the surface ( $\varphi = \pm \frac{\pi}{3}$ ).

#### 4.1.4 H<sub>2</sub>CO admolecule

Like the HCN molecule, the H<sub>2</sub>CO molecule adsorbed on the graphite substrate exhibits six equilibrium sites per hexagon (Figure 2d). The energy minimum  $V_{MG}^m = -208.5$  meV is obtained for the molecule in a flat configuration ( $\theta^e = 90$  deg and  $\chi^e = 90$  deg) with its centre of mass at  $Z = 3.04$  Å on half of the C-C bonds, with a displacement of 0.12 Å inside of the hexagon surface and with its C<sub>2</sub> symmetry axis (z-axis) pointing towards the hexagon site centre.

It should be noted that in its equilibrium sites H<sub>2</sub>CO behaves nearly like HCN with regard to the perpendicular  $\theta$  and parallel  $\varphi$  angular motions of its z-axis, in one hand, but like H<sub>2</sub>O with regard to its spinning motion about this axis.

The energy maximum is  $V_{MG}^M = -186.5$  meV, with the molecule in the flat configuration at  $Z = 3.12$  Å above the hexagon site centre. The surface corrugation energy is then 22 meV.

The saddle point of the diffusion path is obtained for the molecule in the flat configuration at  $Z = 3.04$  Å above the C carbon site with a corresponding energy barrier height  $\Delta V_{MG}(\tau_0)$

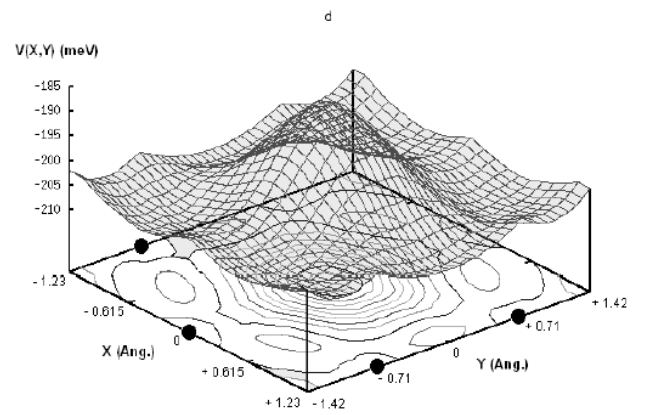
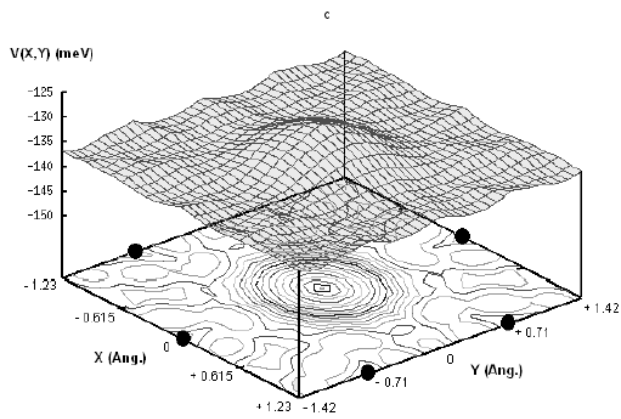
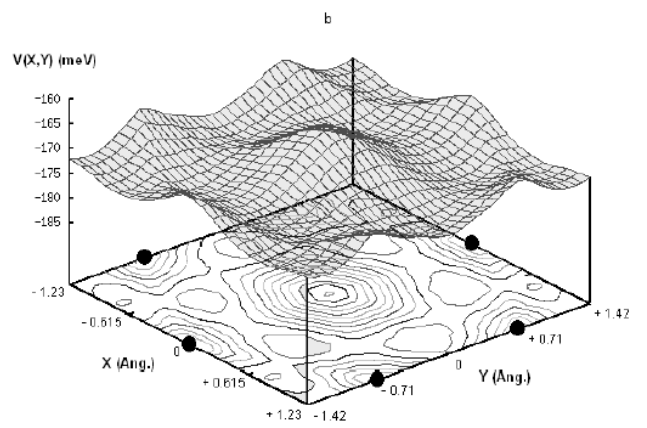
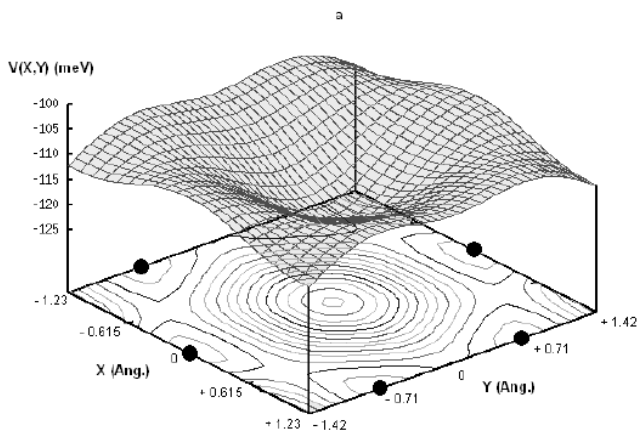


Table 4: Calculated frequencies ( $\text{cm}^{-1}$ ) associated with the translational and orientational oscillations of CO, HCN,  $\text{H}_2\text{O}$  and  $\text{H}_2\text{CO}$  molecules.

Molecule	$\omega_x$	$\omega_y$	$\omega_z$	$\omega_\varphi$	$\omega_\theta$	$\omega_\chi$
CO	26.6	26.6	62.1	$\sim 0$	76.6	-
HCN	21.0	23.4	79.0	32.3	109.7	-
$\text{H}_2\text{O}$	$\sim 0$	$\sim 0$	90.3	22.6	35.5	233.9
$\text{H}_2\text{CO}$	25.0	$\sim 0$	155.7	21.0	91.1	203.3

Table 5: Calculated adsorption energy  $E_a$  (meV) of CO, HCN,  $\text{H}_2\text{O}$  and  $\text{H}_2\text{CO}$  molecules for three typical temperatures.

Molecule	$T = 10 \text{ K}$	$T = 40 \text{ K}$	$T = 100 \text{ K}$
CO	111.3	114.8	114.4
HCN	168.5	163.8	159.5
$\text{H}_2\text{O}$	117.6	123.7	129.6
$\text{H}_2\text{CO}$	181.0	186.6	189.8

= 5 meV (Table 6). Moreover, the rotation of the molecule parallel to the surface plane is a free motion on this site.

We note that the fact that the equilibrium configuration is nearly above the carbon-carbon bonds for HCN,  $\text{H}_2\text{O}$ ,  $\text{H}_2\text{CO}$  molecules results from their strong multipole moments. Their quantum  $V_{\text{LJ}}$ , induction  $V_{\text{I}}$  and electrostatic  $V_{\text{E}}$  contribution parts represent  $\sim 80\%$ ,  $\sim 15\%$  and  $\sim 5\%$ , respectively, of the total potential energy for these molecules.

The weakly polar CO molecule behaves as a quadrupolar molecule and adopts an equilibrium configuration above the hexagon site centre. Its quantum contribution part  $V_{\text{LJ}}$  represents more than  $\sim 95\%$  of the total potential energy.

## 4.2 Adsorption energy calculations

The calculation, using Eq. (12), of the adsorption energy values for single molecules adsorbed on the graphite substrate requires a knowledge of the frequencies  $\omega_s$  associated with the linear and angular oscillations associated with the translational and orientational motions of the molecules around their equilibrium configurations on the most favourable sites.

A discrete variable representation method [32] was used to solve the Schrödinger equation giving the energy levels of a molecule undergoing linear and angular oscillations at its equilibrium site, with the other degrees of freedom being assumed to remain at their equilibrium values. The various frequencies calculated for the molecules treated in this work are reported in table 4.

As can be expected from the potential energy surfaces, the frequencies associated with the orientational motions perpendicular to the surface ( $\theta$  and  $\chi$  motions) (except the  $\theta$  motion for  $\text{H}_2\text{O}$  molecule) are large compared to those associated with the orientational motion parallel to the surface ( $\varphi$  motion).

Finally, the calculated frequencies were introduced into Eq. (12) and the adsorption energies were determined for three typical temperatures. The resulting values are reported in table 5.

Table 6: Calculated surface diffusion constant  $D$  ( $\text{cm}^2/\text{s}$ ) of CO, HCN,  $\text{H}_2\text{O}$  and  $\text{H}_2\text{CO}$  molecules for three typical temperatures.

Molecule	$\frac{m^*}{m}$	$\Delta V_{\text{MG}}(\tau_0)$ (meV)	$T = 10$ K	$T = 40$ K	$T = 100$ K
CO	1.01	12.	$3.3 \times 10^{-10}$	$1. \times 10^{-5}$	$7.3 \times 10^{-5}$
HCN	1.002	13.	$1. \times 10^{-10}$	$1.2 \times 10^{-5}$	$7.2 \times 10^{-5}$
$\text{H}_2\text{O}$	1.11	1.	$1.5 \times 10^{-5}$	$4.3 \times 10^{-5}$	$7.2 \times 10^{-5}$
$\text{H}_2\text{CO}$	1.27	5.	$2.2 \times 10^{-7}$	$1.8 \times 10^{-5}$	$5.1 \times 10^{-5}$

### 4.3 Diffusion constant calculations

The study of the potential energy surface for each adsorbed species allows us to determine the diffusion path, its length  $\lambda$  and potential energy function  $\Delta V_{\text{MG}}(\tau)$ , and the deformation parameters  $\hat{a}_\gamma$  as the molecular diffusion proceeds on the surface.

It must be mentioned that large values for  $\hat{a}_\gamma$  correspond to important equilibrium changes when the molecular centre of mass migrates from the minimum to the saddle point position along the diffusion valley. For instance, the angular deformation parameter values  $\hat{a}_\varphi$  are 1.03 and 0.74  $\text{rad}/\text{\AA}$  for  $\text{H}_2\text{O}$  and  $\text{H}_2\text{CO}$  admolecules, respectively.

In contrast, the angular deformation parameters  $\hat{a}_\theta$  and  $\hat{a}_\chi$  are negligibly small for all the admolecules because of the very weak changes of their perpendicular orientation with respect to the surface during the diffusion motion.

The linear deformation parameter values  $\hat{a}_z$  are 0.10, 0.05, 0.04 and 0.00 for CO, HCN,  $\text{H}_2\text{O}$  and  $\text{H}_2\text{CO}$  admolecules, respectively.

Finally, the possible diffusion paths are indicated in figures 3 and the corresponding energy barrier heights  $\Delta V_{\text{MG}}(\tau_0)$  are given in table 6.

Introducing the calculated deformation parameters in Eq. (15) the mass ratios  $\frac{m^*}{m}$  are obtained and presented in table 6. Note that for the CO and HCN admolecules the mass changes are negligibly small, while for  $\text{H}_2\text{O}$  and  $\text{H}_2\text{CO}$  the effective mass increases by 11% and 27%, respectively.

## 5 Discussion

In the present work we have studied the adsorption of several molecules on a graphite substrate; the molecules were selected because of their biophysical interest, as explained in the introduction.

The major calculation was that of the potential energy surface for each molecule and the figures show the resulting surfaces. A minimization calculation then gave the possible equilibrium positions for each molecule, while the potential energy surface indicated the favourable pathways between these positions which would facilitate surface diffusion of the adsorbed molecule.

The calculated adsorption energies as shown in table 5 show only a relatively weak variation with temperature, although the particular values of the molecule-surface interaction parameters for the HCN molecule lead to a temperature dependence which is in the opposite direction to that for the other three molecules studied.

The calculated diffusion constants for the molecules are shown in table 6 and it is clear that the different saddle point barrier heights and effective masses lead to a variation of several orders of magnitude between the low temperature diffusion constants of the various molecules. In effect, one can remark that at  $T = 10$  K the  $\text{H}_2\text{O}$  molecule could diffuse 3 orders of magnitude more easily than  $\text{H}_2\text{CO}$  and 5 orders of magnitude more easily than CO and HCN molecules.

However, as the temperature increases the thermal energy  $kT$  becomes sufficiently large to overcome the barriers for all the molecules, with the consequence that the diffusion

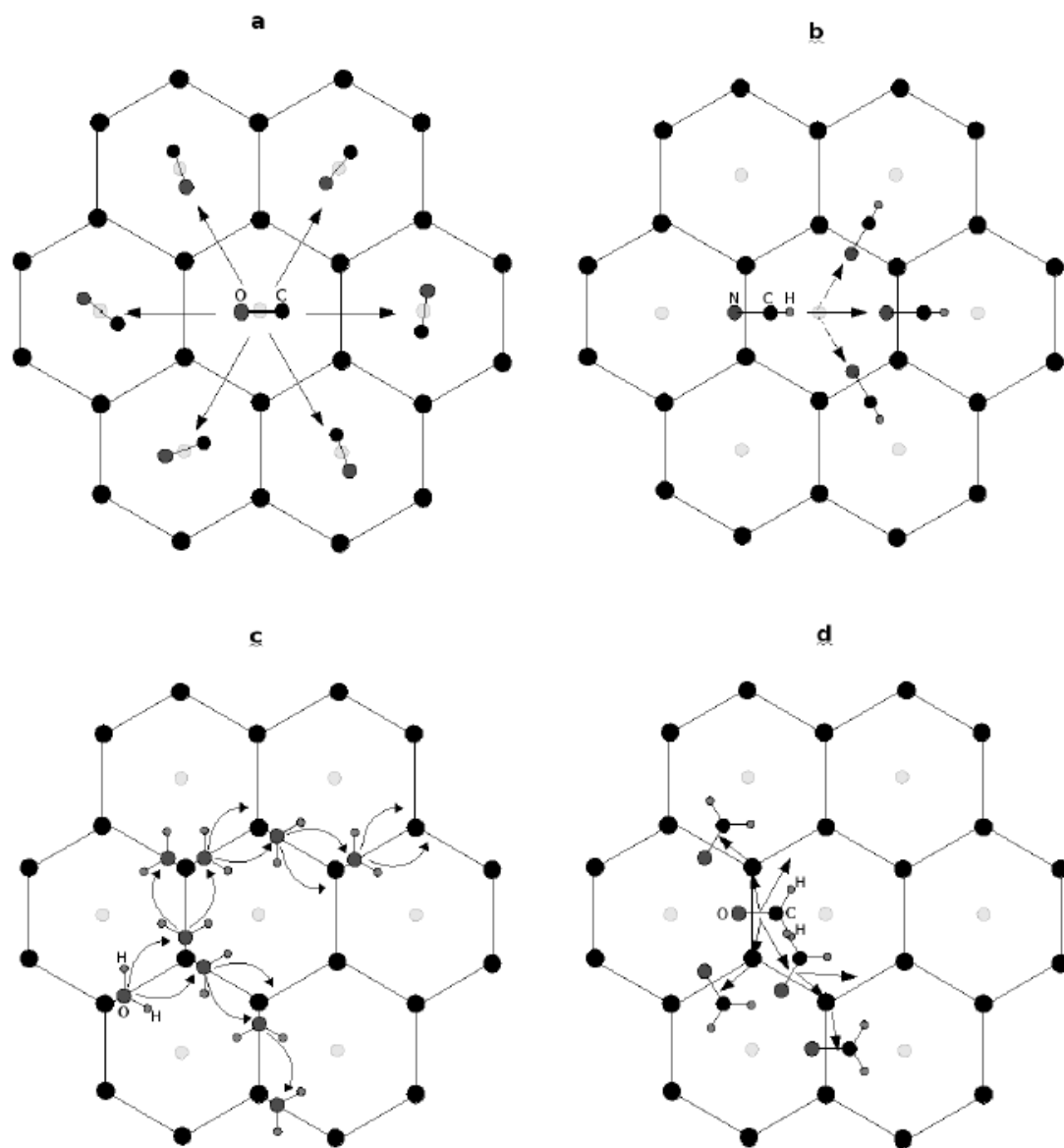


Figure 3: The calculated equilibrium positions for the adsorbed molecule on the graphite substrate, indicating the energetically favoured paths for diffusion between the equilibrium positions. a (CO), b (HCN), c (H<sub>2</sub>O) and d (H<sub>2</sub>CO).

constants vary much less from molecule to molecule as the temperature rises.

## ACKNOWLEDGEMENTS

The authors gratefully acknowledge fruitful discussions with Drs. D. Viennot and S. Picaud.

## Appendix : Rotational matrix transformation

The unitary matrix M characterizing the transformation from the surface absolute frame (O,X,Y,Z) into the molecular one (G,x,y,z) through the Euler angles  $\varphi$ ,  $\theta$  and  $\chi$  is given by [33]

$$M(\varphi, \theta, \chi) = \begin{pmatrix} \cos \varphi \cos \theta \cos \chi - \sin \varphi \sin \chi & \sin \varphi \cos \theta \cos \chi + \cos \varphi \sin \chi & -\sin \theta \cos \chi \\ -\cos \varphi \cos \theta \sin \chi - \sin \varphi \cos \chi & -\sin \varphi \cos \theta \sin \chi + \cos \varphi \cos \chi & \sin \theta \sin \chi \\ \cos \varphi \sin \theta & \sin \varphi \sin \theta & \cos \theta \end{pmatrix}$$

## References

- [1] Draine, B. T. *Astrophys. J.* 1988, *333*, 848.
- [2] Mathis, J. S.; Whiffen, G. *Astrophys. J.* 1989, *341*, 808.
- [3] Watanabe, N.; Kouchi, A. *Astrophys. J. Lett.* 2002, *571*, 173.
- [4] Tielens, A. G. G. M.; Whittet, D. C. B. *in Molecules in Astrophysics*; Ed.; van Dishoeck E. F. (Dordrecht: Kluwer) 1997, 45.
- [5] Bernstein, M. P.; Dworkin, J. P.; Sandford, S. A.; Cooper, G. W.; Allamandola, L. J. *Nature* 2002, *416*, 401.
- [6] Muñoz Caro, G. M.; Meierhenrich, U. J.; Schutte, W. A.; Barbier, B.; Arcones Segovia, A.; Rosenbauer, H.; Thiemann, W. H. P.; Brack, A.; Greenberg, J. M. *Nature* 2002, *416*, 403.
- [7] Woon, D. E. *Astrophys. J. Lett.* 2002, *571*, 177.
- [8] Mendoza, C.; Ruetter, F.; Martorell, G.; Rodríguez, L. S. *Astrophys. J. Lett.* 2004, *601*, 59.
- [9] Vernov, A.; Steele, W. A. *Langmuir* 1992, *8*, 155.
- [10] Gale, R. L.; Beebe, R. A. *J. Phys. Chem.* 1964, *68*, 555.
- [11] Feller, D. *J. Phys. Chem. A* 1999, *103*, 7558.
- [12] Feller, D.; Jordan, K. D. *J. Phys. Chem. A* 2000, *104*, 9971.
- [13] Lin, C. S.; Zhang, R. Q.; Lee, S. T.; Elstner, M.; Frauenheim, Th.; Wan, L. J. *J. Phys. Chem. B* 2005, *109*, 14183.
- [14] Li, S.; Cooper, V. R.; Thonhauser, T.; Puzder, A.; Langreth, D. C. *J. Phys. Chem. A* 2008, *112*, 9031.
- [15] Tsuzuki, S.; Honda, K.; Uchimaru, T.; Mikami, M.; Tanabe, K. *J. Am. Chem. Soc.* 2000, *122*, 11450.
- [16] Zimmerli, U.; Parrinello, M.; Koumoutsakos, P. *J. Chem. Phys.* 2004, *120*, 2693.

- [17] Karapetian, K.; Jordan, K. D. *Water in Confined Environments*; Devlin, J. P.; Buch, V., Eds.; Springer: New York, 2003, 139.
- [18] Avgul, N. N.; Kiselev, A. V. *Chem. Phys. Carbon*; Walker, P. L., Ed.; Dekker: New York, 1970, 6, 1.
- [19] Cheng, B.-M.; Grover, J. R.; Walters, E.A. *Chem. Phys. Lett.* 1995, 232, 364.
- [20] Courty, A.; Mons, M.; Dimicoli, I.; Piuizzi, F.; Gaigeot, M.-P.; Brenner, V.; Pujo, P. d.; Millié, P. *J. Phys. Chem. A* 1998, 102, 6590.
- [21] Lakhlifi, A.; Picaud, S.; Girardet, C.; Allouche, A. *Chem. Phys.* 1995, 201, 73.
- [22] Lakhlifi, A.; Girardet, C. *J. Chem. Phys.* 1996, 105, 2471.
- [23] Lakhlifi, A. *Eur. Phys. J. D* 2000, 8, 211.
- [24] Lakhlifi, A.; Killingbeck, J. P. *J. Phys. Chem. B* 2005, 109, 11322.
- [25] Carlos, W. E.; Cole, M. W. *Surf. Sci.* 1982, 119, 21.
- [26] Vidali, G.; Cole, M. W. *Phys. Rev. B* 1984, 29, 6736.
- [27] Hansen, F. Y.; Bruch, L. W.; Roosevelt, S. E. *Phys. Rev. B* 1992, 45, 11238.
- [28] Hansen, F. Y.; Bruch, L. W. *Phys. Rev. B* 1995, 51, 2515.
- [29] Ionov, S. I.; La Villa, M. E. *J. Chem. Phys.* 1992, 97, 9379.
- [30] Voter, A. F.; Doll, J. D. *J. Chem. Phys.* 1984, 80, 5832.
- [31] Lakhlifi, A.; Girardet, C. *J. Chem. Phys.* 1991, 94, 688.
- [32] Light, J. C.; Hamilton, I. P.; Lill, J. V. *J. Chem. Phys.* 1985, 82, 1400.
- [33] Rose, M. E. *Elementary Theory of Angular Momentum*; Wiley: New York, 1967.